Normative Model and Connectome-Driven Target Prioritization Decision Model for Personalized Precision Modulation of Alzheimer's Disease

Yanqing Dong[1](dongyanqing0078@link.tyut.edu.cn), Yaru Xu[1](2024310105@link.tyut.edu.cn)
Jing Wei[2](20141032@sxufe.edu.cn), Jie Sun[1](sunjie01@tyut.edu.cn)
Xubin Wu[3](wxbwxth0066@gmail.com), Xin Wen[1](xwen@tyut.edu.cn)
Mengni Zhou[1*](zhoumengni@tyut.edu.cn), Jie Xiang[1*](xiangjie@tyut.edu.cn)
[1]Taiyuan University of Technology, Taiyuan, China
[2]Shanxi University of Finance and Economics, Taiyuan, China
[3]Taiyuan University of Science and Technology, Taiyuan, China
[*] corresponding author

Abstract

Transcranial direct current stimulation (tDCS) is a promising non-invasive intervention for Alzheimer's disease (AD). However, current clinical practices rely on generic stimulation targets, which fail to account for individual differences among AD patients, leading to heterogeneous outcomes. To enable personalized neuromodulation, we propose a normative model and connectome-driven target prioritization decision (NCTPD) model. Using a functional connectivity (FC) normative model, we identify each patient's abnormal FC patterns and abnormal regions. We further quantify the coupling strength between candidate targets and abnormal regions via individual structural connectivity (SC), simulating the propagation mechanism of SC-guided current effects to multiple abnormal brain regions, thereby establishing target prioritization. Finally, we perform virtual stimulation on the prioritized targets in the digital twin brain models of 21 AD patients. Higher-ranked targets show more significant regression of abnormal FC toward the normative reference, indicating superior modulation effects. These results validate the effectiveness of the NCTPD model.

Keywords: personalized target selection; Alzheimer's disease; digital twin brain; normative model; transcranial direct current stimulation; virtual stimulation

Introduction

Alzheimer's disease (AD) is a neurodegenerative disorder characterized by progressive cognitive decline, and its progression is often accompanied by impaired interregional information integration and brain network dysfunction (Gaubert et al., 2025; Reijmer et al., 2013). Transcranial direct current stimulation (tDCS), a noninvasive neuromodulation technique, delivers weak direct currents via scalp electrodes to modulate cortical excitability and plasticity, thereby influencing whole-brain network activity and functional connectivity (FC) patterns and offering a potential therapeutic avenue for AD intervention(Gyoda et al., 2025; Woodham et al., 2025). However, most current studies and clinical practice rely on generic, fixed stimulation targets that do not adequately account for inter-individual differences in FC and structural connectivity (SC), resulting in marked heterogeneity in treatment efficacy across individuals(Liu et al., 2025; Yang et al., 2025). Accordingly, optimizing individualized stimulation targets has become a key direction for achieving precision neuromodulatory interventions.

Existing studies frequently use generic stimulation targets to improve group-level FC abnormalities(Jiang et al., 2025). However, previous research has shown that, due to differences in individual pathological states and cognitive symptoms, the FC patterns of AD patients exhibit significant heterogeneity across individuals(Lam et al., 2013). Therefore, generic stimulation targets and group-level abnormal FC patterns fail to adequately account for individual differences in FC, leading to heterogeneous intervention outcomes. As a result, identifying personalized abnormal FC patterns and using them to guide the selection of personalized stimulation targets is key to achieving precise modulation. Previous studies have shown that deviations from normative models of FC can sensitively represent the degree of individual abnormalities and can be used to assess disease severity and identify potential neurobiological subtypes(Marquand et al., 2016; Mito et al., 2025). Huo et al. (2025) quantified AD neurophysiological heterogeneity by utilizing deviations from dynamic functional connectivity group norms, and further explored the correlation between these patterns and clinical indicators, providing new insights for personalized identification of AD abnormal FC patterns and personalized precision intervention.

Although directly selecting stimulation targets based on abnormal patterns in AD can modulate local functional networks(Koch et al., 2022), this approach is overly focused on individual abnormal brain regions and may fail to activate key large-scale functional networks associated with the disease, limiting the precision of the intervention. Prior studies have shown that tDCS effects are not confined to the stimulation target but propagate along SC pathways coupled with the target, thereby inducing widespread brain-wide functional reorganization(Dong et al., 2025; Xie et al., 2025). Therefore, using SC as a "navigation" system enables more precise guidance of current effects to multiple associated abnormal brain regions, facilitating broad intervention on complex FC patterns. However, AD patients exhibit significant individual neurophysiological heterogeneity, and group-level SC templates often fail to accurately capture the SC damage in specific individuals, making it difficult to predict the propagation path of stimulation effects in particular pathological contexts. Therefore, combining individualized functional abnormalities with SC constraints to select targets will be key to enhancing

In G. Boleda, I. Dautriche, M. Maldonado, C. Saldana and T. Torrent (Eds.), *Proceedings of the 48th Annual Conference of the Cognitive Science Society*

the effectiveness of AD modulation.

In this work, we propose a normative model and connectome-driven target prioritization decision (NCTPD) model for AD. The model first establishes a normative model based on the FC of the normal control (NC) group and quantifies the individual abnormal FC patterns in AD patients, which are then used as targets for modulation. Next, we identify abnormal regions within the abnormal FC patterns and quantify the structural coupling strength between each candidate region and the abnormal regions under the constraint of SC to determine target priority. Finally, stimulation is applied to the target regions in a personalized digital twin brain model, predicting the changes in FC, and the target efficacy is assessed by the regression magnitude of the normative deviation. This methodology enables personalized target selection under FC normative deviation and structural constraints, providing a strategy for future model-guided closed-loop optimization of neuromodulation targets.

Methods

We propose an individualized neuromodulation target-prioritization decision model for AD constrained by FC normative model and SC connectome. The FC normative model delineates the distributed dysfunctional regions requiring modulation by identifying individual-specific abnormal patterns; meanwhile, the SC connectome leverages physical topology to guide the propagation of stimulation effects along the structural backbone, thereby ensuring that single-target stimulation effectively covers and synergistically modulates these multiple abnormal regions. As shown in Figure 1, first, identifying abnormal FC patterns in AD subjects through FC normative deviation; second, performing target prioritization under functional-structural connectivity constraints; and third, evaluating the efficacy of prioritized targets through virtual stimulation. This methodology provides a quantitative individualized target ranking, avoiding extensive trial-and-error, and offers methodological support for the development and closed-loop optimization of precision neuromodulation strategies for AD.

Identification of abnormal FC patterns

To characterize the individualized abnormal FC patterns in patients with AD, we established an edge-wise FC normative space based on a digital-twin brain framework. This workflow comprises two core steps: first, constructing a digital-twin brain to reproduce the dynamical features of empirical brain activity; and subsequently, establishing a normative model based on the simulated FC from the NC group to quantify the standardized deviations of each AD individual relative to the norm.

Digital twin brain. We construct a large-scale brain network model comprising multiple neural masses as a digital-twin brain to simulate dynamic brain activity. The neural-mass formulation adopts the dMFM proposed by Deco et al. (2013) to capture local cortical dynamics, while inter-regional coupling is governed by SC. In this model, each cortical region is represented by coupled excitatory and inhibitory spiking populations, whose dynamics are described by the following equations:

$$\dot{S}_i = -\frac{S_i}{\tau_S} + \gamma(1 - S_i)H(x_i) + \sigma\xi_i(t), \tag{1}$$

$$x_i = wJS_i + GJ\sum_j C_{ij}S_j + I, \tag{2}$$

$$H(x_i) = \frac{ax_i - b}{1 - \exp[-d(ax_i - b)]}. \tag{3}$$

Here, $\dot{S}_i$, x_i, and $H(x_i)$ denote the mean synaptic gating variable, the total input current, and the mean firing rate of the neuronal population in cortical region i, respectively. Model parameters were taken from neurophysiological measurements to ensure biophysical realism (Gordon et al., 2017). Detailed definitions of these parameters, as well as the fitting procedure for large-scale dynamical models, have been reported in prior work(Wei et al., 2022). Based on the resulting digital-twin brain, we are able to reproduce group-level dynamical features in both AD and NC cohorts and to generate simulated FC that closely matches empirical FC while preserving its complexity and biological plausibility.

Normative modeling of FC. We construct the normative space based on the FC of NC subjects generated by the digital twin brain. Specifically, for each NC subject s, the FC matrix generated by the digital twin brain is first Fisher z-transformed and vectorized by extracting the upper triangular elements. To avoid treating multiple simulations from the same subject as independent samples, which could introduce bias in statistical analysis and incorrectly inflate the sample size, we average the repeated simulations within each NC subject to obtain the representative edge connectivity strength $C_{s,r}^{NC}$. We then estimate the normative mean and standard deviation for each edge r across the NC group:

$$\mu_r^{NC} = \frac{1}{|NC|}\sum_{s\in NC} C_{s,r}^{NC}, \tag{4}$$

$$\sigma_r^{NC} = \sqrt{\frac{1}{|NC|-1}\sum_{s\in NC}\left(C_{s,r}^{NC} - \mu_r^{NC}\right)^2}. \tag{5}$$

This yields the edge-wise FC normative parameters $\mu_r^{NC}, \sigma_r^{NC}$, which serve as a unified statistical reference for calculating subject deviations in AD.

Individualized abnormal FC patterns in AD. For the FC of AD individual s simulated by the digital-twin brain model, we apply the same preprocessing pipeline as that used for the NC group to obtain the edge-wise FC strength $C_{s,r}^{AD}$. Based on the previously estimated NC edge-wise normative parameters $\{\mu_r^{NC}, \sigma_r^{NC}\}_{r=1}^{E}$, the standardized deviation $Z_{s,r}^{AD}$ of AD individual s on edge r is defined as:

$$Z_{s,r}^{AD} = \frac{C_{s,r}^{AD} - \mu_r^{NC}}{\sigma_r^{NC}}, \qquad r = 1, \ldots, E. \tag{6}$$

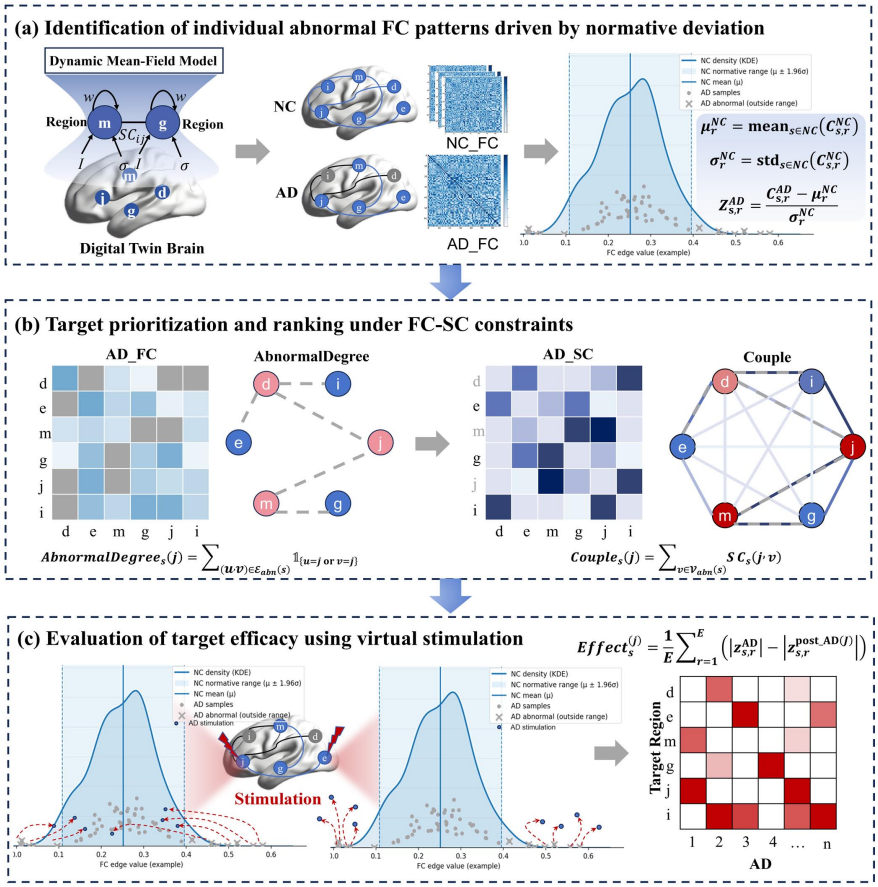

Figure 1: The normative model and connectome-driven target prioritization decision (NCTPD) model. (a) Identification of individual abnormal FC patterns driven by normative model deviation. (b) Target prioritization and ranking under FC-SC constraints. (c) Evaluation of target efficacy using virtual stimulation.

To construct individualized abnormal FC patterns, we adopt a deviation-magnitude–based Top-p edge selection strategy. Specifically, all FC edges are ranked in descending order according to $|Z^{AD}_{s,r}|$, and the top 2% are selected to form the abnormal FC pattern $\mathcal{E}_{abn}(s)$ for AD individual s. These abnormal FC patterns are then used as targets for evaluating and optimizing neuromodulation effects.

Functional–structural connectivity constrained target prioritization

To devise more precise individualized stimulation strategies, we propose a target decision model constrained by both FC and SC, leveraging the structural propagation mechanism of tDCS. Specifically, the model first delineates individualized functionally dysfunctional regions based on abnormal patterns; subsequently, it quantifies the physical modulation potential of candidate nodes over these regions using the structural connectome, serving as the basis for target prioritization.

Individualized abnormal brain regions in AD. Abnormal degree is used to quantify the extent to which a brain region is involved in an individual's abnormal FC pattern. For any candidate node $j \in \{1, 2, \ldots, n\}$, its abnormal degree is defined as the number of times it appears as an endpoint in the abnormal edge set $\mathcal{E}_{abn}(s)$:

$$\text{AbnormalDegree}_s(j) = \sum_{(u,v)\in\mathcal{E}_{abn}(s)} \mathbb{1}_{\{u=j \text{ or } v=j\}}. \quad (7)$$

Here, $\mathbb{1}_{\{u=j \text{ or } v=j\}}$ is an indicator function that checks whether the abnormal edge (u, v) has node j as one of its endpoints: it takes the value 1 if either $u = j$ or $v = j$, and 0 otherwise. A larger $\text{AbnormalDegree}_s(j)$ indicates that region j plays a more prominent role in the abnormal FC pattern of AD individual s, thereby defining the set of individual abnormal regions $\mathcal{V}_{abn}(s)$.

Structural connectome guided target prioritization. Based on the physical mechanism of tDCS propagation along structural pathways, we introduce "structural coupling strength" to quantify the modulation potential of candidate targets over the set of abnormal brain regions $\mathcal{V}_{abn}(s)$. Specifically, given the structural connectivity matrix $\mathbf{SC}_s \in \mathbb{R}^{n\times n}$ for individual s, the structural coupling strength for any candidate target j is defined as:

$$Couple_s(j) = \sum_{v \in \mathcal{V}_{abn}(s)} SC_s(j, v). \tag{8}$$

Here, $SC_s(j, v)$ denotes the normalized SC weight between region j and abnormal region v. We use $Couple_s(j)$ as the target priority score. A larger $Couple_s(j)$ indicates a stronger overall SC between target j and the set of abnormal nodes. From a structural propagation perspective, such targets are more likely to cover and influence abnormal regions, and therefore, are expected to yield more pronounced improvements in the abnormal FC pattern.

Evaluation of target prioritization based on virtual stimulation

Based on the obtained target-priority sequence, we sequentially apply virtual stimulation to each candidate target in the AD digital-twin brain model and simulate the network response post-stimulation. Furthermore, the modulation effect is quantified by comparing the deviations of the AD individual's FC abnormal pattern from the normative reference before and after stimulation, thereby validating the effectiveness of the proposed target-prioritization strategy.

Virtual stimulation. Using the trained digital-twin brain model, we perturb each candidate target to simulate the brain dynamics induced by electrical stimulation and obtain stimulation-evoked changes in FC. Specifically, we introduce an exogenous perturbation term to the mean synaptic gating variable of the stimulated region in the digital-twin brain model, as described in Equation 9:

$$\dot{S}_i' = -\frac{S_i}{\tau_S} + \gamma(1 - S_i)H(x_i) + \sigma\xi_i(t) + \delta(i, t). \tag{9}$$

Here, $\dot{S}_i'$ denotes the rate of change of the mean synaptic gating variable after perturbation, and $\delta(i, t)$ represents the stimulation intensity applied to region i at time t. Each virtual stimulation targets a single region at a time, while all other regions remain unperturbed.

Evaluation of target improvement effect. To validate the effectiveness of the target-prioritization decision model, we evaluate the improvement of targets by comparing the deviation changes of FC relative to the normative reference before and after targeted stimulation in the AD digital-twin brain model. Specifically, for each candidate stimulation target $j \in \{1, 2, \ldots, n\}$, virtual stimulation is applied with brain region j serving as the stimulation site. The FC matrix obtained from each simulation is processed using the same preprocessing pipeline as the normative model, and the results from multiple simulations are averaged at the individual level to obtain the post-stimulation mean edge-strength vector $\mathbf{C}_{s,r}^{\text{post\_AD(j)}}$. Under the unified FC normative parameters $\{\mu_r^{NC}, \sigma_r^{NC}\}_{r=1}^{E}$, the edge-wise standardized deviation in the post-stimulation state is defined as:

$$Z_{s,r}^{post\_AD(j)} = \frac{C_{s,r}^{post\_AD(j)} - \mu_r^{NC}}{\sigma_r^{NC}}, \qquad r = 1, \ldots, E. \tag{10}$$

Further, based on the deviation representations relative to the FC normative reference before and after stimulation, we define stimulation-induced modulation effects to quantify the extent to which abnormal FC is driven toward the norm under stimulation. The modulation effect of an AD individual is defined as:

$$\text{Effect}_s^{(j)} = \frac{1}{E} \sum_{r=1}^{E} \left(\left| Z_{s,r}^{\text{AD}} \right| - \left| Z_{s,r}^{\text{post\_AD}(j)} \right| \right). \tag{11}$$

If $Effect_s^{(j)} > 0$, it indicates that the deviation magnitude of the connection relative to the FC norm decreases after stimulation, suggesting that the connection state returns to the norm and the modulation effect is significant; if $Effect_s^{(j)} < 0$, it indicates that the deviation magnitude increases, suggesting insufficient modulation effect and potentially leading to disease deterioration.

Datasets

We used the Alzheimer's Disease Neuroimaging Initiative (ADNI) dataset (http://adni.loni.usc.edu/), which includes subjects with AD ($n = 21$) and NC ($n = 29$). These participants underwent multimodal imaging, including rs-fMRI, T1-weighted imaging, and diffusion tensor imaging (DTI). All rs-fMRI data were acquired using a 3T MRI scanner with TR = 3 s, providing 187 time points per subject. For the rs-fMRI data, the brain was parcellated into 68 regions based on the Desikan-Killiany brain atlas.

Results

Individual abnormal FC patterns in AD

First, the average fitting correlations between the empirical and simulated FC of the digital twin brains reached $r = 0.35 \pm 0.10$ for the AD group and $r = 0.39 \pm 0.05$ for the NC group, confirming that the digital twin brain accurately reproduces the empirical FC features of the subjects and providing a reliable basis for subsequent analyses. The spatial distribution of abnormal edges in three randomly selected AD subjects, referenced to the FC normative model, is shown in Figure 2. As illustrated, there is significant topological heterogeneity in abnormal edges across individuals: the abnormal connectivity in AD_Sub01 is mainly concentrated in the bilateral frontal and anterior cingulate regions, particularly involving the orbitofrontal and mid-frontal cortices. In contrast, AD_Sub03 exhibits a broader distribution, extending beyond the frontal areas to involve the bilateral paracentral lobule and right precentral gyrus. Finally, AD_Sub08's abnormal connectivity shows the most extensive involvement, spanning the bilateral frontal and parietal regions (specifically the precuneus and superior parietal lobule), as well as the left temporal cortex. These abnormal connections are primarily located

in the frontal, parietal, and temporal regions, which are considered key pathological areas in AD(Chauveau et al., 2025). Therefore, it is evident that the FC deviations in AD do not follow a single, unified pattern, but instead present individual-specific abnormal FC patterns.

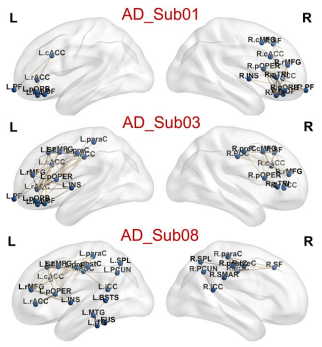

Figure 2: Personalized abnormal FC patterns in AD.

Personalized target selection and neuromodulation effect improvement in AD

Figure 3a shows the top 10 personalized stimulation targets for three AD subjects. The results indicate that, although the targets vary slightly across subjects, the majority of the targets are confined to the left hemisphere of the brain. This suggests that the left hemisphere may play a dominant role in the functional modulation of AD, potentially linked to specific pathological features and functional connectivity shifts.

We conducted virtual stimulation on 68 personalized stimulation targets for 21 AD subjects using a personalized digital twin brain model and quantitatively evaluated the neuromodulation effects (Figure 3b). The results show significant individual differences in the virtual stimulation responses across subjects. Targets ranked higher consistently exhibited stable positive modulation effects across multiple subjects. In contrast, a few targets demonstrated negative modulation effects, suggesting that stimulation of these targets may have adverse effects on the FC of the corresponding subjects' brains.

At the group level, we calculated the mean and median of the modulation effect distribution for each rank to represent central tendency, and used the standard deviation to describe the dispersion and individual differences across subjects. As shown in Figure 3c, the stimulation effect decreased as the target rank moved lower. Targets ranked higher showed higher modulation effect values in both the group mean and median, indicating that these targets more effectively reduce the deviation of abnormal edges from the FC normative model and promote the regression of abnormal patterns toward the normative reference. As the rank moved lower, the effect gradually diminished, and in some cases, the effect approached zero or became negative, suggesting that the improvement diminished significantly, with some targets possibly exacerbating deviations.

We further analyzed the improvement effects on the abnormal edge set for each subject's top 10 targets (Top-10) and bottom 10 targets (Bottom-10) (Figure 3d), revealing that the improvement effects of the Top-10 were significantly superior to those of the Bottom-10 ($p < 0.05$, paired t-tests). The individual-level comparison (Figure 3e) also showed that the Top-10 improvement effects were better than the Bottom-10 for the majority of subjects, further validating the effectiveness and practical value of the model in personalized neuromodulation target selection.

Commonalities and Differences in Personalized Target Selection for AD

We further calculated the frequency of occurrence of different brain regions in the Top-10 high-priority targets across 21 AD subjects to characterize the commonalities and differences in target selection at the group level. As shown in Figure 4, several brain regions appeared repeatedly in the Top-10 lists of multiple subjects, including the banks of the superior temporal sulcus (BSTS), inferior parietal lobule (IPL), entorhinal cortex (ENT), rostral anterior cingulate cortex (cACC), inferior temporal gyrus (ITG), fusiform gyrus (FUS), cuneus (CUN), and rostral middle frontal gyrus (cMFG). This indicates that, despite significant heterogeneity in the individualized ranking, certain brain regions are consistently prioritized across subjects, suggesting that their modulation of abnormal FC patterns may have stronger generalizability.

Moreover, we found that these high-frequency modulation targets were all located in the left hemisphere of the brain. Previous studies have shown that the pattern of left-sided lateralization decreases as AD progresses (Srivishagan et al., 2020; Wang et al., 2023). Functional asymmetry is a fundamental organizational principle of the human brain, with each hemisphere supporting distinct cognitive functions to enhance the parallel processing of multiple tasks, thereby improving overall processing efficiency (Corballis, 2019; Hartwigsen et al., 2021; Vallortigara, Rogers, et al., 2005). Compared to healthy elderly individuals, the left hemisphere in AD patients exhibits more pronounced changes, including reduced cortical thickness (Roe et al., 2021), impaired metabolism or blood flow (Loewenstein et al., 1989; Weise et al., 2018), and network dropout in memory tasks (Tyrer et al., 2020). Stimulation of certain brain regions in the left hemisphere may help compensate for the functional loss of key neural regions involved in specific cognitive processes (Kumar et al., 2017). Therefore, we speculate that stimulation of the left hemisphere may enhance FC, and repetitive stimulation may promote structural plasticity, ultimately contributing to the improvement of cognitive function in patients.

Conclusion

In this study, to address the heterogeneity of therapeutic efficacy arising from the use of generic stimulation targets in clinical interventions for AD, we proposed a target prioritization decision model that integrates a FC normative model with

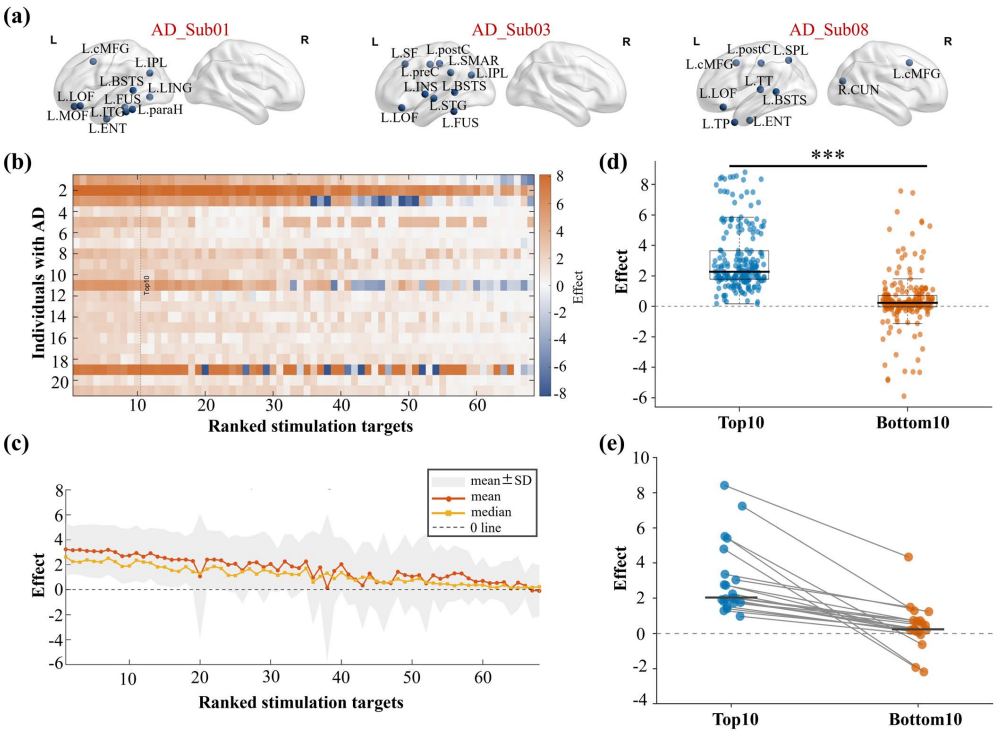

Figure 3: Personalized stimulation targets and modulation effect improvement in AD. (a) Personalized stimulation targets in AD. (b) Modulation effect improvement of personalized targets. (c) Average modulation effect improvement of personalized targets across subjects. (d) Improvement effects of Top-10 vs. Bottom-10 targets.(e) Individual-level improvement effects of Top-10 vs. Bottom-10 targets.

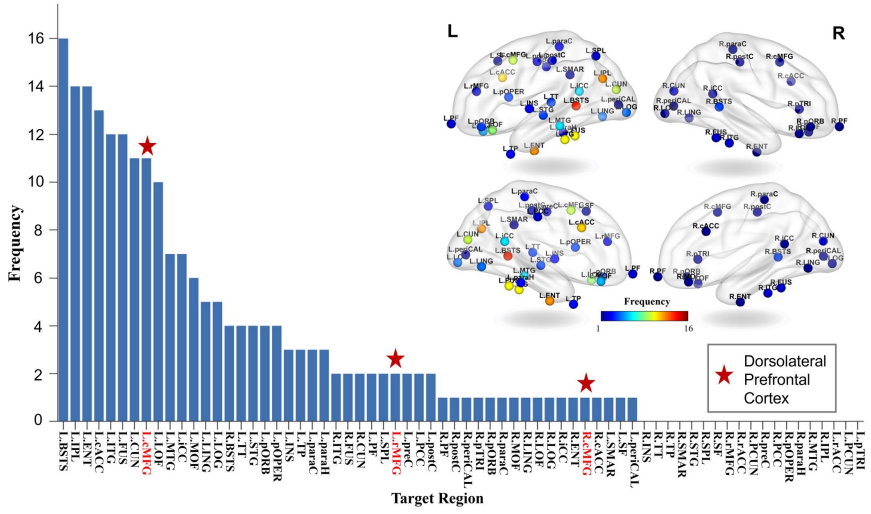

Figure 4: High-frequency brain regions in personalized stimulation targets.

a SC connectome to derive personalized stimulation targets for AD. First, individual abnormal FC patterns and abnormal brain regions were identified using an FC normative model. Subsequently, the coupling strength between candidate targets and abnormal regions was computed based on SC and used to rank stimulation targets. Finally, virtual stimulation was performed within a digital twin brain model to evaluate the degree of post-stimulation FC regression toward the normative reference. The results demonstrated that the proposed model effectively optimized individualized target selection, providing a computational framework and strategic support for precision neuromodulation in AD.

Acknowledgments

This work was supported by the following grants: the National Natural Science Foundation of China 62376184 (Jie Xiang), Central Guided Local Science and Technology Development Project YDZJSX20231A017 (Jie Xiang), Shanxi Provincial Special Guidance Program for the Transformation of Scientific and Technological Achievements 202404021301032 (Jie Xiang), the National Natural Science Foundation of China 62303445 (Mengni Zhou), 62206196 (Xin Wen).

References

Chauveau, L., Landeau, B., Dautricourt, S., Turpin, A.-L., Delarue, M., Hébert, O., de La Sayette, V., Chételat, G., & de Flores, R. (2025). Anterior-temporal network hyperconnectivity is key to alzheimer's disease: From ageing to dementia. *Brain*, *148*(6), 2008–2022.

Corballis, M. C. (2019). Evolution of cerebral asymmetry. *Progress in brain research*, *250*, 153–178.

Deco, G., Ponce-Alvarez, A., Mantini, D., Romani, G. L., Hagmann, P., & Corbetta, M. (2013). Resting-state functional connectivity emerges from structurally and dynamically shaped slow linear fluctuations. *Journal of Neuroscience*, *33*(27), 11239–11252.

Dong, Y., Wei, J., Peng, S., Wu, X., Xu, Y., Feng, J., Zhang, J., Jirsa, V., & Xiang, J. (2025). Effects of tdcs of the dlpfc on brain networks: A hybrid brain modeling study. *PLOS Computational Biology*, *21*(9), e1013486.

Gaubert, S., Garces, P., Hipp, J., Bruña, R., Lopéz, M. E., Maestu, F., Vaghari, D., Henson, R., Paquet, C., & Engemann, D.-A. (2025). Exploring the neuromagnetic signatures of cognitive decline from mild cognitive impairment to alzheimer's disease dementia. *EBioMedicine*, *114*.

Gordon, E. M., Laumann, T. O., Gilmore, A. W., Newbold, D. J., Greene, D. J., Berg, J. J., Ortega, M., Hoyt-Drazen, C., Gratton, C., Sun, H., Hampton, J. M., Coalson, R. S., Nguyen, A. L., McDermott, K. B., Shimony, J. S., Snyder, A. Z., Schlaggar, B. L., Petersen, S. E., Nelson, S. M., & Dosenbach, N. U. (2017). Precision functional mapping of individual human brains. *Neuron*, *95*(4), 791–807.e7.

Gyoda, T., Hashimoto, R., Inagaki, S., Tsushi, N., Kitao, T., Minati, L., & Yoshimura, N. (2025). Electroencephalography-guided transcranial direct current stimulation improves picture-naming performance. *NeuroImage*, *308*, 120997.

Hartwigsen, G., Bengio, Y., & Bzdok, D. (2021). How does hemispheric specialization contribute to human-defining cognition? *Neuron*, *109*(13), 2075–2090.

Huo, Y., Jing, R., Li, P., Chen, P., Si, J., Liu, G., & Liu, Y. (2025). Delineating the heterogeneity of alzheimer's disease and mild cognitive impairment using normative models of dynamic brain functional networks. *Biological Psychiatry*, *97*(11), 1034–1044.

Jiang, L., Fung, C. C. S., & Cheng, C. P. W. (2025). Research advances in neuronavigated target localization for repetitive transcranial magnetic stimulation in depression: From standardization to individualized neuromodulation. *Frontiers in Neuroimaging*, *4*, 1703198.

Koch, G., Casula, E. P., Bonnì, S., Borghi, I., Assogna, M., Minei, M., Pellicciari, M. C., Motta, C., D'Acunto, A., Porrazzini, F., et al. (2022). Precuneus magnetic stimulation for alzheimer's disease: A randomized, sham-controlled trial. *Brain*, *145*(11), 3776–3786.

Kumar, S., Zomorrodi, R., Ghazala, Z., Blumberger, D., Fischer, C., Daskalakis, Z., Mulsant, B., Pollock, B., & Rajji, T. (2017). 361. dorsolateral prefrontal cortex neuroplasticity deficits in alzheimer's disease. *Biological Psychiatry*, *81*(10), S148.

Lam, B., Masellis, M., Freedman, M., Stuss, D. T., & Black, S. E. (2013). Clinical, imaging, and pathological heterogeneity of the alzheimer's disease syndrome. *Alzheimer's research & therapy*, *5*(1), 1.

Liu, B., Hu, C., & Bao, P. (2025). Precision tms through the integration of neuroimaging and machine learning: Optimizing stimulation targets for personalized treatment. *Frontiers in Human Neuroscience*, *19*, 1682852.

Loewenstein, D. A., Barker, W. W., Chang, J.-Y., Apicella, A., Yoshii, F., Kothari, P., Levin, B., & Duara, R. (1989). Predominant left hemisphere metabolic dysfunction in dementia. *Archives of Neurology*, *46*(2), 146–152.

Marquand, A. F., Rezek, I., Buitelaar, J., & Beckmann, C. F. (2016). Understanding heterogeneity in clinical cohorts using normative models: Beyond case-control studies. *Biological Psychiatry*, *80*(7), 552–561.

Mito, R., Cole, J. H., Genc, S., Jackson, G. D., & Zalesky, A. (2025). Towards precision mri biomarkers in epilepsy with normative modelling. *Brain*, awaf090.

Reijmer, Y. D., Leemans, A., Caeyenberghs, K., Heringa, S. M., Koek, H. L., Biessels, G. J., & Group, U. V. C. I. S. (2013). Disruption of cerebral networks and cognitive impairment in alzheimer disease. *Neurology*, *80*(15), 1370–1377.

Roe, J. M., Vidal-Piñeiro, D., Sørensen, Ø., Brandmaier, A. M., Düzel, S., Gonzalez, H. A., Kievit, R. A., Knights, E., Kühn, S., Lindenberger, U., et al. (2021). Asymmetric thinning of the cerebral cortex across the adult lifespan is accelerated in alzheimer's disease. *Nature Communications*, *12*(1), 721.

Srivishagan, S., Perera, A. A. I., Hojjat, A., Ratnarajah, N., & Initiative, A. D. N. (2020). Brain network measures for groups of nodes: Application to normal aging and alzheimer's disease. *Brain Connectivity*, *10*(6), 316–327.

Tyrer, A., Gilbert, J. R., Adams, S., Stiles, A. B., Bankole, A. O., Gilchrist, I. D., & Moran, R. J. (2020). Lateralized memory circuit dropout in alzheimer's disease patients. *Brain Communications*, *2*(2), fcaa212.

Vallortigara, G., Rogers, L. J., et al. (2005). Survival with an asymmetrical brain: Advantages and disadvantages of cerebral lateralization. *Behavioral and Brain Sciences*, *28*(4), 575–588.

Wang, L., Du, T., Zhao, L., Shi, Y., & Zeng, W. (2023). Research on the lateralization of brain functional complexity in mild cognitive impairment-alzheimer's disease progression based on multiscale lateralized brain entropy. *Biomedical Signal Processing and Control*, *86*, 105216.

Wei, J., Wang, B., Yang, Y., Niu, Y., Yang, L., Guo, Y., & Xiang, J. (2022). Effects of virtual lesions on temporal dynamics in cortical networks based on personalized dynamic models. *NeuroImage*, *254*, 119087.

Weise, C. M., Chen, K., Chen, Y., Kuang, X., Savage, C. R., Reiman, E. M., Initiative, A. D. N., et al. (2018). Left lateralized cerebral glucose metabolism declines in amyloid-β positive persons with mild cognitive impairment. *NeuroImage: Clinical*, *20*, 286–296.

Woodham, R. D., Selvaraj, S., Lajmi, N., Hobday, H., Sheehan, G., Ghazi-Noori, A.-R., Lagerberg, P. J., Rizvi, M., Kwon, S. S., Orhii, P., et al. (2025). Home-based transcranial direct current stimulation treatment for major depressive disorder: A fully remote phase 2 randomized sham-controlled trial. *Nature Medicine*, *31*(1), 87–95.

Xie, K., Sahlas, E., Ngo, A., Chen, J., Arafat, T., Royer, J., Zhou, Y., Rodríguez-Cruces, R., Dascal, A., Caldairou, B., et al. (2025). Personalized biomarkers of multiscale functional alterations in temporal lobe epilepsy. *Nature Communications*, *16*(1), 10145.

Yang, C., Wang, P., Zhu, Z., Wu, H., Su, Q., Zhu, S., Shao, Y., Lin, H., & Biswal, B. B. (2025). Individualized functional connectome biomarkers predict clinical symptoms after rtms treatment in alzheimer's disease. *Translational Psychiatry*, AddedOnReleaseOfVoR–CitationID.